

# Exclusive semileptonic and nonleptonic decays of $B$ mesons to orbitally excited light mesons

D. Ebert<sup>1</sup>, R. N. Faustov<sup>1,2</sup> and V. O. Galkin<sup>1,2</sup>

<sup>1</sup> *Institut für Physik, Humboldt-Universität zu Berlin,  
Newtonstr. 15, D-12489 Berlin, Germany*

<sup>2</sup> *Dorodnicyn Computing Centre, Russian Academy of Sciences,  
Vavilov Str. 40, 119991 Moscow, Russia*

The form factors of weak decays of the  $B$  meson to orbitally excited scalar, axial vector and tensor light mesons are calculated in the framework of the QCD-motivated relativistic quark model based on the quasipotential approach. Relativistic effects are systematically taken into account. The form factors are expressed through the overlap integrals of the meson wave functions and their dependence on the momentum transfer is selfconsistently determined in the whole kinematical range. On this basis semileptonic and two-body nonleptonic  $B$  decay rates to orbitally excited light mesons are calculated. Good agreement of the obtained predictions with available experimental data is found.

PACS numbers: 13.20.He, 12.39.Ki

## I. INTRODUCTION

Recently significant experimental progress has been achieved in studying weak decays of  $B$  mesons into light mesons [1]. Many new decay modes have been measured including nonleptonic decays involving excited light mesons [2–5]. In Ref. [6] we investigated semileptonic  $B$  decays to the ground state  $\pi$  and  $\rho$  mesons in the framework of the relativistic quark model based on the quasipotential approach in QCD. The peculiar feature of the heavy-to-light weak decays is the very broad kinematical range in which the recoil momentum of the final light meson is significantly larger than the mass of the light meson except the small region near the point of zero recoil. Therefore it is very important to take into account all relevant relativistic effects and determine the decay form factors without any extrapolations or additional parameterizations. Weak decay form factors were selfconsistently calculated [6] in the whole accessible kinematical range. It was found that both the behaviour of the form factors on momentum transfer and differential and total semileptonic decay rates agree well with the rather precise experimental data. This allowed us to determine the Cabibbo-Kobayashi-Maskawa (CKM) matrix element  $V_{ub}$ .

In this paper we further extend our analysis for the consideration of the weak semileptonic and two-body nonleptonic  $B$  decays to the orbitally excited light mesons. We calculate the corresponding decay form factors paying special attention for a consistent account of all relativistic effects and determination of the form factor dependence on the momentum transfer in the whole accessible kinematical range. For calculations we use masses and wave functions of orbitally excited light mesons which were previously studied by us in Ref. [7]. Table I quotes a comparison of our predictions for the  $P$ -wave light unflavoured mesons with

TABLE I: Predicted [7] and measured masses of the  $P$ -wave light ( $q = u, d$ ) unflavored mesons (in MeV).

$n^{2S+1}L_J$	$J^{PC}$	Theory $q\bar{q}$	Experiment [1]			
			$I = 1$	mass	$I = 0$	mass
$1^3P_0$	$0^{++}$	1176	$a_0$	1474(19)	$f_0$	1200-1500
$1^3P_1$	$1^{++}$	1254	$a_1$	1230(40)	$f_1$	1281.8(6)
$1^3P_2$	$2^{++}$	1317	$a_2$	1318.3(6)	$f_2$	1275.1(12)
$1^1P_1$	$1^{+-}$	1258	$b_1$	1229.5(3.2)	$h_1$	1170(20)

experimental data [1]. Results for scalar  $a_0$ ,  $f_0$ , spin triplet ( $^3P_1$ ) axial vector  $a_1$ ,  $f_1$ , spin singlet ( $^1P_1$ ) axial vector  $b_1$ ,  $h_1$  and tensor  $a_2$ ,  $f_2$  mesons are presented. Our model predicts [7] the light scalar meson masses heavier than 1 GeV. The scalar mesons below 1 GeV are well described as the light tetraquarks, composed from the light scalar diquarks and antidiquarks [8]. From Table I we see that the calculated mass of the scalar  $q\bar{q}$  state  $1^3P_0$  is significantly lower than the mass of the experimentally observed  $a_0(1450)$  meson. Our model predicts that this state is also the tetraquark composed from the axial vector diquark and antidiquark with the mass 1480 MeV [8]. Nevertheless, for the purpose of comparison, we here assume that the lightest scalar  $q\bar{q}$  state corresponds to the  $a_0(1450)$  meson and test this assumption by confronting the obtained predictions for the  $B$  decays involving this meson with available experimental data and results of the different theoretical investigations based on quark models, sum rules, light cone sum rules and perturbative QCD. Therefore the study of weak  $B$  decays involving light scalars is an important problem, since it can help to reveal their real nature.

The calculated weak decay form factors are used for the evaluation of the semileptonic  $B$  decay branching fractions. Then they are employed for studying the two-body nonleptonic  $B$  decays using the factorization approach. Such approximation significantly simplifies calculations, since it expresses the matrix elements of the weak Hamiltonian responsible for the nonleptonic decays through the product of the transition matrix elements and meson decay constants. Comparison of the obtained results with experimental data, which are mostly available for the nonleptonic  $B$  decays involving light axial vector mesons [3, 4], can help in testing this approach and discriminate between different models for form factors.

## II. RELATIVISTIC QUARK MODEL

In the quasipotential approach a meson is described as a bound quark-antiquark state with a wave function satisfying the quasipotential equation of the Schrödinger type

$$\left( \frac{b^2(M)}{2\mu_R} - \frac{\mathbf{p}^2}{2\mu_R} \right) \Psi_M(\mathbf{p}) = \int \frac{d^3q}{(2\pi)^3} V(\mathbf{p}, \mathbf{q}; M) \Psi_M(\mathbf{q}), \quad (1)$$

where the relativistic reduced mass is

$$\mu_R = \frac{E_1 E_2}{E_1 + E_2} = \frac{M^4 - (m_1^2 - m_2^2)^2}{4M^3}, \quad (2)$$

and  $E_1, E_2$  are the center of mass energies on mass shell given by

$$E_1 = \frac{M^2 - m_2^2 + m_1^2}{2M}, \quad E_2 = \frac{M^2 - m_1^2 + m_2^2}{2M}. \quad (3)$$

Here  $M = E_1 + E_2$  is the meson mass,  $m_{1,2}$  are the quark masses, and  $\mathbf{p}$  is their relative momentum. In the center of mass system the relative momentum squared on mass shell reads

$$b^2(M) = \frac{[M^2 - (m_1 + m_2)^2][M^2 - (m_1 - m_2)^2]}{4M^2}. \quad (4)$$

The kernel  $V(\mathbf{p}, \mathbf{q}; M)$  in Eq. (1) is the quasipotential operator of the quark-antiquark interaction. It is constructed with the help of the off-mass-shell scattering amplitude, projected onto the positive energy states. Constructing the quasipotential of the quark-antiquark interaction, we have assumed that the effective interaction is the sum of the usual one-gluon exchange term with the mixture of long-range vector and scalar linear confining potentials, where the vector confining potential contains the Pauli interaction. The quasipotential is then defined by [7]

$$V(\mathbf{p}, \mathbf{q}; M) = \bar{u}_1(p)\bar{u}_2(-p)\mathcal{V}(\mathbf{p}, \mathbf{q}; M)u_1(q)u_2(-q), \quad (5)$$

with

$$\mathcal{V}(\mathbf{p}, \mathbf{q}; M) = \frac{4}{3}\alpha_s D_{\mu\nu}(\mathbf{k})\gamma_1^\mu\gamma_2^\nu + V_{\text{conf}}^V(\mathbf{k})\Gamma_1^\mu\Gamma_{2;\mu} + V_{\text{conf}}^S(\mathbf{k}),$$

where  $\alpha_s$  is the QCD coupling constant,  $D_{\mu\nu}$  is the gluon propagator in the Coulomb gauge

$$D^{00}(\mathbf{k}) = -\frac{4\pi}{\mathbf{k}^2}, \quad D^{ij}(\mathbf{k}) = -\frac{4\pi}{k^2} \left( \delta^{ij} - \frac{k^i k^j}{\mathbf{k}^2} \right), \quad D^{0i} = D^{i0} = 0, \quad (6)$$

and  $\mathbf{k} = \mathbf{p} - \mathbf{q}$ . Here  $\gamma_\mu$  and  $u(p)$  are the Dirac matrices and spinors

$$u_i^\lambda(p) = \sqrt{\frac{\epsilon_i(p) + m_i}{2\epsilon_i(p)}} \begin{pmatrix} 1 \\ \frac{\boldsymbol{\sigma}\mathbf{p}}{\epsilon_i(p) + m_i} \end{pmatrix} \chi^\lambda, \quad (7)$$

where  $\boldsymbol{\sigma}$  and  $\chi^\lambda$  are Pauli matrices and spinors and  $\epsilon_i(p) = \sqrt{\mathbf{p}^2 + m_i^2}$ . The effective long-range vector vertex is given by

$$\Gamma_\mu(\mathbf{k}) = \gamma_\mu + \frac{i\kappa}{2m}\sigma_{\mu\nu}k^\nu, \quad (8)$$

where  $\kappa$  is the Pauli interaction constant characterizing the long-range anomalous chromomagnetic moment of quarks. Vector and scalar confining potentials in the nonrelativistic limit reduce to

$$\begin{aligned} V_{\text{conf}}^V(r) &= (1 - \varepsilon)(Ar + B), \\ V_{\text{conf}}^S(r) &= \varepsilon(Ar + B), \end{aligned} \quad (9)$$

reproducing

$$V_{\text{conf}}(r) = V_{\text{conf}}^S(r) + V_{\text{conf}}^V(r) = Ar + B, \quad (10)$$

where  $\varepsilon$  is the mixing coefficient.

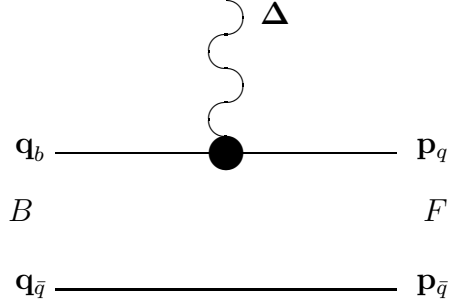


FIG. 1: Lowest order vertex function  $\Gamma_\mu^{(1)}(\mathbf{p}, \mathbf{q})$  contributing to the current matrix element (11).

The expression for the quasipotential of the heavy quarkonia, expanded in  $v^2/c^2$  can be found in Ref. [9]. The quasipotential for the heavy quark interaction with a light antiquark without employing the nonrelativistic ( $v/c$ ) expansion is given in Refs. [7, 10]. All the parameters of our model like quark masses, parameters of the linear confining potential  $A$  and  $B$ , mixing coefficient  $\varepsilon$  and anomalous chromomagnetic quark moment  $\kappa$  are fixed from the analysis of heavy quarkonium masses and radiative decays [9]. The quark masses  $m_b = 4.88$  GeV,  $m_c = 1.55$  GeV,  $m_s = 0.5$  GeV,  $m_{u,d} = 0.33$  GeV and the parameters of the linear potential  $A = 0.18$  GeV<sup>2</sup> and  $B = -0.30$  GeV have values inherent for quark models. The value of the mixing coefficient of vector and scalar confining potentials  $\varepsilon = -1$  has been determined from the consideration of the heavy quark expansion for the semileptonic  $B \rightarrow D$  decays [11] and charmonium radiative decays [9]. Finally, the universal Pauli interaction constant  $\kappa = -1$  has been fixed from the analysis of the fine splitting of heavy quarkonia  $^3P_J$ - states [9] and the heavy quark expansion for semileptonic decays of heavy mesons [11] and baryons [12]. Note that the long-range magnetic contribution to the potential in our model is proportional to  $(1 + \kappa)$  and thus vanishes for the chosen value of  $\kappa = -1$  in accordance with the flux tube model.

### III. MATRIX ELEMENTS OF THE ELECTROWEAK CURRENT

In order to calculate the exclusive semileptonic decay rate of the  $B$  meson, it is necessary to determine the corresponding matrix element of the weak current between meson states. In the quasipotential approach, the matrix element of the weak current  $J_\mu^W = \bar{q}\gamma_\mu(1 - \gamma_5)b$ , associated with the  $b \rightarrow q$  transition, between a  $B$  meson with mass  $M_B$  and momentum  $p_B$  and a final  $P$ -wave light meson  $F$  with mass  $M_F$  and momentum  $p_F$  takes the form [13]

$$\langle F(p_F) | J_\mu^W | B(p_B) \rangle = \int \frac{d^3p d^3q}{(2\pi)^6} \bar{\Psi}_{F \mathbf{p}_F}(\mathbf{p}) \Gamma_\mu(\mathbf{p}, \mathbf{q}) \Psi_{B \mathbf{p}_B}(\mathbf{q}), \quad (11)$$

where  $\Gamma_\mu(\mathbf{p}, \mathbf{q})$  is the two-particle vertex function and  $\Psi_{M \mathbf{p}_M}$  are the meson ( $M = B, F$ ) wave functions projected onto the positive energy states of quarks and boosted to the moving reference frame with momentum  $\mathbf{p}_M$ .

The contributions to  $\Gamma_\mu(\mathbf{p}, \mathbf{q})$  come from Figs. 1 and 2. The leading order vertex function  $\Gamma_\mu^{(1)}(\mathbf{p}, \mathbf{q})$  corresponds to the impulse approximation, while the vertex function  $\Gamma_\mu^{(2)}(\mathbf{p}, \mathbf{q})$  accounts for contributions of the negative-energy states. Note that the form of the relativistic corrections emerging from the vertex function  $\Gamma_\mu^{(2)}(\mathbf{p}, \mathbf{q})$  explicitly depends on the Lorentz

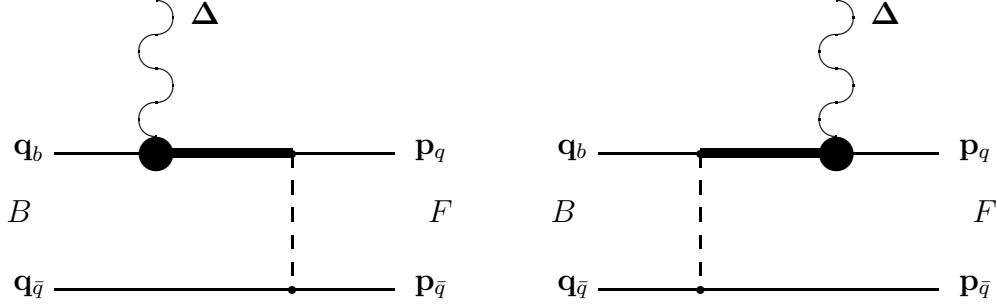


FIG. 2: Vertex function  $\Gamma_\mu^{(2)}(\mathbf{p}, \mathbf{q})$  taking the quark interaction into account. Dashed lines correspond to the effective potential  $\mathcal{V}$  in (5). Bold lines denote the negative-energy part of the quark propagator.

structure of the quark-antiquark interaction. In the leading order of the  $v^2/c^2$  expansion for  $B$  and  $F$  only  $\Gamma_\mu^{(1)}(\mathbf{p}, \mathbf{q})$  contributes, while  $\Gamma_\mu^{(2)}(\mathbf{p}, \mathbf{q})$  contributes at the subleading order. The vertex functions look like

$$\Gamma_\mu^{(1)}(\mathbf{p}, \mathbf{q}) = \bar{u}_q(p_q)\gamma_\mu(1 - \gamma^5)u_b(q_b)(2\pi)^3\delta(\mathbf{p}_{\bar{q}} - \mathbf{q}_{\bar{q}}), \quad (12)$$

and

$$\begin{aligned} \Gamma_\mu^{(2)}(\mathbf{p}, \mathbf{q}) = & \bar{u}_q(p_q)\bar{u}_{\bar{q}}(p_{\bar{q}})\left\{\gamma_{1\mu}(1 - \gamma_1^5)\frac{\Lambda_b^{(-)}(k)}{\epsilon_b(k) + \epsilon_b(p_q)}\gamma_1^0\mathcal{V}(\mathbf{p}_{\bar{q}} - \mathbf{q}_{\bar{q}})\right. \\ & \left. + \mathcal{V}(\mathbf{p}_{\bar{q}} - \mathbf{q}_{\bar{q}})\frac{\Lambda_q^{(-)}(k')}{\epsilon_q(k') + \epsilon_q(q_b)}\gamma_1^0\gamma_{1\mu}(1 - \gamma_1^5)\right\}u_b(q_b)u_{\bar{q}}(q_{\bar{q}}), \end{aligned} \quad (13)$$

where the superscripts “(1)” and “(2)” correspond to Figs. 1 and 2, the subscripts  $q, \bar{q}, b$  are the quark indices,  $\mathbf{k} = \mathbf{p}_q - \Delta$ ;  $\mathbf{k}' = \mathbf{q}_b + \Delta$ ;  $\Delta = \mathbf{p}_F - \mathbf{p}_B$ ;

$$\Lambda_i^{(-)}(p) = \frac{\epsilon_i(p) - (m_i\gamma^0 + \gamma^0(\boldsymbol{\gamma}\mathbf{p}))}{2\epsilon_i(p)}.$$

Here the quark momenta are expressed through relative momenta  $\mathbf{q}$  and  $\mathbf{p}$  as follows [13]

$$\begin{aligned} p_{q(\bar{q})} &= \epsilon_{q(\bar{q})}(p)\frac{p_F}{M_F} \pm \sum_{i=1}^3 n^{(i)}(p_F)p^i, \\ q_{b(\bar{q})} &= \epsilon_{b(\bar{q})}(q)\frac{p_B}{M_B} \pm \sum_{i=1}^3 n^{(i)}(p_B)q^i, \end{aligned}$$

and  $n^{(i)}$  are three four-vectors given by

$$n^{(i)\mu}(p) = \left\{ \frac{p^i}{M}, \delta_{ij} + \frac{p^i p^j}{M(E + M)} \right\}, \quad E = \sqrt{\mathbf{p}^2 + M^2}.$$

The wave function of a final  $P$ -wave  $F$  meson at rest is given by

$$\Psi_F(\mathbf{p}) \equiv \Psi_{F(2S+1P_J)}^{JM}(\mathbf{p}) = \mathcal{Y}_S^{JM} \psi_{F(2S+1P_J)}(p), \quad (14)$$

where  $J$  and  $\mathcal{M}$  are the total meson angular momentum and its projection, while  $S = 0, 1$  is the total spin.  $\psi_{F(2S+1P_J)}(p)$  is the radial part of the wave function, which has been determined by the numerical solution of Eq. (1) in [7, 10]. The spin-angular momentum part  $\mathcal{Y}_S^{J\mathcal{M}}$  has the following form

$$\mathcal{Y}_S^{J\mathcal{M}} = \sum_{\sigma_1\sigma_2} \langle 1 \mathcal{M} - \sigma_1 - \sigma_2, S \sigma_1 + \sigma_2 | J \mathcal{M} \rangle \langle \frac{1}{2} \sigma_1, \frac{1}{2} \sigma_2 | S \sigma_1 + \sigma_2 \rangle Y_1^{\mathcal{M} - \sigma_1 - \sigma_2} \chi_1(\sigma_1) \chi_2(\sigma_2). \quad (15)$$

Here  $\langle j_1 m_1, j_2 m_2 | J \mathcal{M} \rangle$  are the Clebsch-Gordan coefficients,  $Y_l^m$  are spherical harmonics, and  $\chi(\sigma)$  (where  $\sigma = \pm 1/2$ ) are spin wave functions,

$$\chi(1/2) = \begin{pmatrix} 1 \\ 0 \end{pmatrix}, \quad \chi(-1/2) = \begin{pmatrix} 0 \\ 1 \end{pmatrix}.$$

It is important to note that the wave functions entering the weak current matrix element (11) are not in the rest frame in general. For example, in the  $B$  meson rest frame ( $\mathbf{p}_B = 0$ ), the final meson is moving with the recoil momentum  $\mathbf{\Delta}$ . The wave function of the moving meson  $\Psi_{F\mathbf{\Delta}}$  is connected with the wave function in the rest frame  $\Psi_{F\mathbf{0}} \equiv \Psi_F$  by the transformation [13]

$$\Psi_{F\mathbf{\Delta}}(\mathbf{p}) = D_q^{1/2}(R_{L\mathbf{\Delta}}^W) D_{\bar{q}}^{1/2}(R_{L\mathbf{\Delta}}^W) \Psi_{F\mathbf{0}}(\mathbf{p}), \quad (16)$$

where  $R^W$  is the Wigner rotation,  $L_{\mathbf{\Delta}}$  is the Lorentz boost from the meson rest frame to a moving one, and the rotation matrix  $D_q^{1/2}(R)$  in spinor representation is given by

$$\begin{pmatrix} 1 & 0 \\ 0 & 1 \end{pmatrix} D_q^{1/2}(R_{L\mathbf{\Delta}}^W) = S_q^{-1}(\mathbf{p}_q) S_q(\mathbf{\Delta}) S_q(\mathbf{p}), \quad (17)$$

where

$$S_q(\mathbf{p}) = \sqrt{\frac{\epsilon_q(p) + m_q}{2m_q}} \left( 1 + \frac{\boldsymbol{\alpha}\mathbf{p}}{\epsilon_q(p) + m_q} \right)$$

is the usual Lorentz transformation matrix of the four-spinor.

#### IV. FORM FACTORS OF THE SEMILEPTONIC $B$ DECAYS TO THE ORBITALLY EXCITED LIGHT MESONS

The matrix elements of the weak current  $J_\mu^W = \bar{b}\gamma_\mu(1 - \gamma_5)q$  for  $B$  decays to orbitally excited scalar light mesons ( $S$ ) can be parametrized by two invariant form factors [14]

$$\langle S(p_F) | \bar{q}\gamma^\mu b | B(p_B) \rangle = 0,$$

$$\langle S(p_F) | \bar{q}\gamma^\mu \gamma_5 b | B(p_B) \rangle = f_+(q^2) (p_B^\mu + p_F^\mu) + f_-(q^2) (p_B^\mu - p_F^\mu), \quad (18)$$

where four-momentum transfer  $q = p_B - p_F$ ,  $M_S$  is the scalar meson mass.

The matrix elements of the weak current for  $B$  decays to the spin triplet ( ${}^3P_1$ ) axial vector mesons ( $AV$ ) can be expressed in terms of four invariant form factors [14]

$$\langle A(p_F) | \bar{q}\gamma^\mu b | B(p_B) \rangle = (M_B + M_A) h_{V_1}(q^2) \epsilon^{*\mu} + [h_{V_2}(q^2) p_B^\mu + h_{V_3}(q^2) p_F^\mu] \frac{\epsilon^* \cdot q}{M_B}, \quad (19)$$

$$\langle A(p_F) | \bar{q}\gamma^\mu \gamma_5 b | B(p_B) \rangle = \frac{2ih_A(q^2)}{M_B + M_A} \epsilon^{\mu\nu\rho\sigma} \epsilon_\nu^* p_{B\rho} p_{F\sigma}, \quad (20)$$

where  $M_A$  and  $\epsilon^\mu$  are the mass and polarization vector of the axial vector meson. The matrix elements of the weak current for  $B$  decays to the spin singlet ( $^1P_1$ ) axial vector mesons are obtained from Eqs. (19) by the replacement of the set of form factors  $h_i(q^2)$  by  $g_i(q^2)$  ( $i = V_1, V_2, V_3, A$ ).

The matrix elements of the weak current for  $B$  decays to tensor mesons ( $T$ ) can be decomposed in four Lorentz-invariant structures [14]

$$\langle T(p_F) | \bar{q} \gamma^\mu b | B(p_B) \rangle = \frac{2it_V(q^2)}{M_B + M_T} \epsilon^{\mu\nu\rho\sigma} \epsilon_{\nu\alpha}^* \frac{p_B^\alpha}{M_B} p_{B\rho} p_{F\sigma}, \quad (21)$$

$$\begin{aligned} \langle T(p_F) | \bar{q} \gamma^\mu \gamma_5 b | B(p_B) \rangle &= (M_B + M_T) t_{A_1}(q^2) \epsilon^{*\mu\alpha} \frac{p_{B\alpha}}{M_B} \\ &+ [t_{A_2}(q^2) p_B^\mu + t_{A_3}(q^2) p_F^\mu] \epsilon_{\alpha\beta}^* \frac{p_B^\alpha p_B^\beta}{M_B^2}, \end{aligned} \quad (22)$$

where  $M_T$  and  $\epsilon^{\mu\nu}$  are the mass and polarization tensor of the tensor meson.

The general structure of the current matrix element (11) is rather complicated, since it is necessary to integrate both with respect to  $d^3p$  and  $d^3q$ . We calculate exactly the contribution of the leading vertex function  $\Gamma_\mu^{(1)}(\mathbf{p}, \mathbf{q})$  given by Eq. (12) to the transition matrix element of the weak current (11) using the  $\delta$ -function. As a result the contribution of  $\Gamma_\mu^{(1)}(\mathbf{p}, \mathbf{q})$  to the current matrix element has the usual structure of an overlap integral of meson wave functions and can be calculated exactly in the whole kinematical range. The calculation of the subleading contribution  $\Gamma_\mu^{(2)}(\mathbf{p}, \mathbf{q})$  is significantly more difficult. The heavy quark is present in the initial  $B$  meson only. Therefore the expansion in its inverse powers retains the dependence on the relative momentum in the energy of the final light quark. Such dependence does not allow one to perform one of the integrals in the decay matrix element (11) using the quasipotential equation. However the final light meson has a large recoil momentum ( $\mathbf{\Delta} \equiv \mathbf{p}_F - \mathbf{p}_B$ ,  $|\mathbf{\Delta}_{\max}| = (M_B^2 - M_F^2)/(2M_B) \sim 2.5$  GeV) almost in the whole kinematical range except the small region near  $q^2 = q_{\max}^2$  ( $|\mathbf{\Delta}| = 0$ ). This also means that the recoil momentum of the final meson is large with respect to the mean relative quark momentum  $|\mathbf{p}|$  in the meson ( $\sim 0.5$  GeV). Thus one can neglect  $|\mathbf{p}|$  compared to  $|\mathbf{\Delta}|$  in the final light quark energy  $\epsilon_q(p + \mathbf{\Delta}) \equiv \sqrt{m_q^2 + (\mathbf{p} + \mathbf{\Delta})^2}$ , replacing it by  $\epsilon_q(\mathbf{\Delta}) \equiv \sqrt{m_q^2 + \mathbf{\Delta}^2}$  in expressions for the  $\Gamma_\mu^{(2)}(\mathbf{p}, \mathbf{q})$ . This replacement removes the relative momentum dependence in the energy of the light quark and thus permits to perform one of the integrations in the  $\Gamma_\mu^{(2)}(\mathbf{p}, \mathbf{q})$  contribution using the quasipotential equation. This contribution is relatively small, since it is proportional to the binding energy in the meson. To demonstrate this observation, we show in Fig. 3 leading  $h_A^{(1)}(q^2)$  and subleading  $h_A^{(2)}(q^2)$  terms of the form factor  $h_A(q^2)$  as an example. Contributions of such terms to other form factors are similar. Therefore application of heavy quark and large recoil energy expansions and the extrapolation of the subleading contribution to the small recoil region introduces minor errors. Similar calculations for the weak  $B$  decays to light ground state mesons were made in Ref. [6]. There it was shown that such extrapolation introduces uncertainties from the vicinity of zero recoil  $q^2 = q_{\max}^2$  of less than 1%. It is important to emphasize that calculating the form factors we consistently take into account all relativistic contributions including the boosts of the meson wave functions from the rest reference frame to the moving ones, given by Eq. (16). Recently we performed the similar calculation of the weak form factors for the transitions of  $B_c$  mesons to the orbitally excited mesons [14]. Since in this calculation the spectator charmed quark was treated without the  $1/m_c$  expansion and the

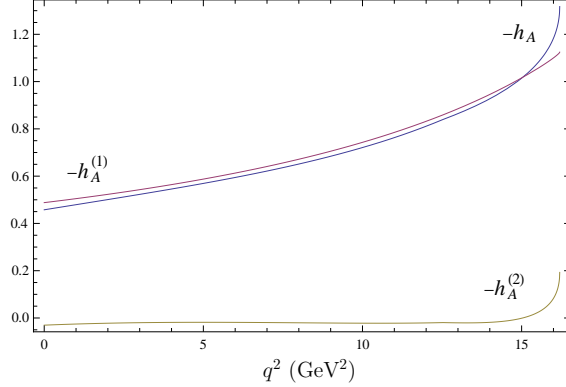


FIG. 3: The form factor  $h_A(q^2)$  of the  $B \rightarrow a_1$  weak transition with leading  $h_A^{(1)}(q^2)$  and subleading  $h_A^{(2)}(q^2)$  contributions.

final active quark was considered to be light in the framework of the approach described above, we can use for the present calculation the expressions for the decay form factors given in Appendix of Ref. [14] with obvious replacements. In the limits of infinitely heavy quark mass and large recoil energy of the final meson, these form factors satisfy all heavy quark symmetry relations [15, 16].

For numerical evaluations of the form factors we use the quasipotential wave functions of the  $B$  meson and orbitally excited light mesons obtained in [7, 10]. Our results for the masses of these mesons are given in Table I. With the exception of the  $a_0$  meson they are in good agreement with available experimental data [1].

In Fig. 4 we plot form factors of the weak  $B$  transitions to the isovector  $P$ -wave light mesons (scalar  $a_0$ , axial vector  $a_1$  and  $b_1$ , tensor  $a_2$ ). The calculated values of these form factors at  $q^2 = 0$ , several intermediate points and  $q^2 = q_{\text{max}}^2 \equiv (M_B - M_F)^2$  are given in Table II. Since we do not distinguish between isovector and isoscalar mesons, the form factors for the corresponding weak decays involving isoscalar mesons coincide with the isovector ones up to the factor  $1/\sqrt{2}$ , which comes from the flavour function of the light neutral meson. As it was argued above, the main source of the uncertainties of our form factor calculations originates from the subleading terms (13). We can conservatively estimate the error arising from the application of the heavy quark expansion and the extrapolation of the subleading contributions to the small recoil region to be less than 1% in the interval  $q^2 = 0 \div 14 \text{ GeV}^2$  and to be less than 4% for the interval  $q^2 = 14 \text{ GeV}^2 \div q_{\text{max}}^2$ .

These form factors can be approximated with good accuracy by the following expressions:

$$(a) \quad F(q^2) = f_+(q^2), f_-(q^2), h_A(q^2), h_{V_3}(q^2), g_{V_1}(q^2), g_{V_2}(q^2), g_{V_3}(q^2), t_V(q^2), t_{A_1}(q^2), t_{A_2}(q^2), t_{A_3}(q^2)$$

$$F(q^2) = \frac{F(0)}{\left(1 + \sigma_1 \frac{q^2}{M_B^2} + \sigma_2 \frac{q^4}{M_B^4} + \sigma_3 \frac{q^6}{M_B^6} + \sigma_4 \frac{q^8}{M_B^8}\right)}, \quad (23)$$

$$(b) \quad F(q^2) = h_{V_1}(q^2), h_{V_2}(q^2), g_A(q^2)$$

$$F(q^2) = 2F(0) - \frac{F(0)}{\left(1 + \sigma_1 \frac{q^2}{M_B^2} + \sigma_2 \frac{q^4}{M_B^4} + \sigma_3 \frac{q^6}{M_B^6} + \sigma_4 \frac{q^8}{M_B^8}\right)}, \quad (24)$$



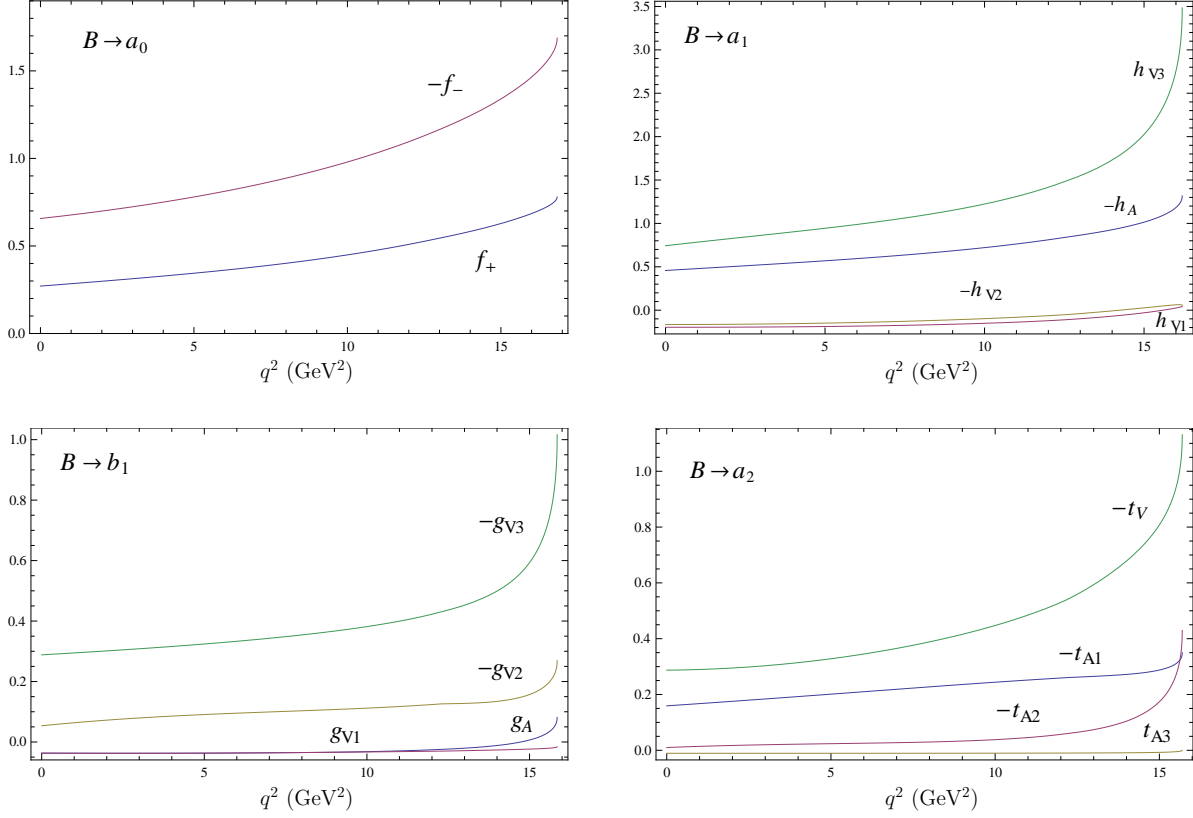


FIG. 4: Form factors of the  $B$  decays to the  $P$ -wave light mesons.

TABLE II: Calculated values of the form factors of the  $B$  decays to the  $P$ -wave light mesons at  $q^2 = 0$ , several intermediate points and  $q^2 = q_{\max}^2 \equiv (M_B - M_F)^2$ .

$q^2$	$B \rightarrow a_0$		$B \rightarrow a_1$				$B \rightarrow b_1$				$B \rightarrow a_2$			
	$f_+$	$f_-$	$h_A$	$h_{V_1}$	$h_{V_2}$	$h_{V_3}$	$g_A$	$g_{V_1}$	$g_{V_2}$	$g_{V_3}$	$t_V$	$t_{A_1}$	$t_{A_2}$	$t_{A_3}$
0	0.27	-0.66	-0.46	-0.20	0.17	0.74	-0.04	-0.04	-0.05	-0.29	-0.29	-0.16	-0.01	-0.01
2.5	0.31	-0.71	-0.51	-0.20	0.16	0.84	-0.04	-0.04	-0.08	-0.31	-0.30	-0.18	-0.02	-0.01
5	0.35	-0.78	-0.57	-0.19	0.15	0.94	-0.04	-0.04	-0.09	-0.32	-0.33	-0.20	-0.02	-0.01
7.5	0.39	-0.87	-0.64	-0.17	0.13	1.06	-0.04	-0.04	-0.10	-0.35	-0.38	-0.22	-0.03	-0.01
10	0.45	-0.98	-0.72	-0.15	0.10	1.22	-0.03	-0.03	-0.11	-0.38	-0.45	-0.24	-0.04	-0.01
12.5	0.53	-1.13	-0.84	-0.11	0.05	1.48	-0.02	-0.03	-0.13	-0.44	-0.56	-0.26	-0.06	-0.01
15	0.63	-1.35	-1.02	-0.03	-0.02	2.05	0.01	-0.02	-0.16	-0.60	-0.82	-0.29	-0.18	-0.01
$q_{\max}^2$	0.78	-1.69	-1.32	0.04	-0.06	3.48	0.08	-0.02	-0.27	-1.02	-1.13	-0.35	-0.43	0

where the values  $F(0)$  are given in Table II and the values  $\sigma_i$  ( $i = 1, 2, 3, 4$ ) are given in Table III.<sup>1</sup> In the next sections we apply the obtained form factors for the calculation of semileptonic and nonleptonic  $B$  decays involving orbitally excited light mesons.

<sup>1</sup> Note that we do not use these parameterizations for further calculations.

TABLE III: Fitted parameters of form factor parameterizations (23) and (24).

	$B \rightarrow a_0$		$B \rightarrow a_1$			$B \rightarrow b_1$				$B \rightarrow a_2$				
	$f_+$	$f_-$	$h_A$	$h_{V_1}$	$h_{V_2}$	$h_{V_3}$	$g_A$	$g_{V_1}$	$g_{V_2}$	$g_{V_3}$	$t_V$	$t_{A_1}$	$t_{A_2}$	$t_{A_3}$
$\sigma_1$	-1.20	-0.63	-0.91	0.04	-0.15	-0.53	1.20	-0.95	-3.04	0.72	0.98	-0.89	-4.25	-1.33
$\sigma_2$	-0.27	-2.29	-2.40	-1.59	-1.85	-7.10	-12.5	9.71	2.46	-14.3	-14.7	-4.04	7.39	16.9
$\sigma_3$	2.35	6.03	9.36	0.36	-0.82	23.9	38.1	-30.9	13.5	45.5	36.8	17.0	-3.10	-63.9
$\sigma_4$	-2.53	-5.34	-9.90	-0.93	2.52	-24.2	-41.7	37.1	-22.2	-46.4	-31.8	-17.4	-3.69	77.1

## V. SEMILEPTONIC $B$ DECAYS TO ORBITALLY EXCITED LIGHT MESONS

The differential decay rate for the  $B$  meson decay to  $P$ -wave light mesons reads [17]

$$\frac{d\Gamma(B \rightarrow F(S, AV, T)l\bar{\nu})}{dq^2} = \frac{G_F^2}{(2\pi)^3} |V_{ub}|^2 \frac{\lambda^{1/2}(q^2 - m_l^2)^2}{24M_B^3 q^2} \left[ HH^\dagger \left( 1 + \frac{m_l^2}{2q^2} \right) + \frac{3m_l^2}{2q^2} H_t H_t^\dagger \right], \quad (25)$$

where  $G_F$  is the Fermi constant,  $V_{ub}$  is the CKM matrix element,  $\lambda \equiv \lambda(M_B^2, M_F^2, q^2) = M_B^4 + M_F^4 + q^4 - 2(M_B^2 M_F^2 + M_F^2 q^2 + M_B^2 q^2)$ ,  $m_l$  is the lepton mass and

$$HH^\dagger \equiv H_+ H_+^\dagger + H_- H_-^\dagger + H_0 H_0^\dagger. \quad (26)$$

The helicity components  $H_\pm$ ,  $H_0$  and  $H_t$  of the hadronic tensor are expressed through the invariant form factors.

(a)  $B \rightarrow S(^3P_0)$  transition

$$\begin{aligned} H_\pm &= 0, \\ H_0 &= \frac{\lambda^{1/2}}{\sqrt{q^2}} f_+(q^2), \\ H_t &= \frac{1}{\sqrt{q^2}} [(M_B^2 - M_S^2) f_+(q^2) + q^2 f_-(q^2)]. \end{aligned} \quad (27)$$

(b)  $B \rightarrow AV(^3P_1)$  transition

$$\begin{aligned} H_\pm &= (M_B + M_{AV}) h_{V_1}(q^2) \pm \frac{\lambda^{1/2}}{M_B + M_{AV}} h_A, \\ H_0 &= \frac{1}{2M_{AV} \sqrt{q^2}} \left\{ (M_B + M_{AV})(M_B^2 - M_{AV}^2 - q^2) h_{V_1}(q^2) + \frac{\lambda}{2M_B} [h_{V_2}(q^2) + h_{V_3}(q^2)] \right\}, \\ H_t &= \frac{\lambda^{1/2}}{2M_{AV} \sqrt{q^2}} \left\{ (M_B + M_{AV}) h_{V_1}(q^2) + \frac{M_B^2 - M_{AV}^2}{2M_B} [h_{V_2}(q^2) + h_{V_3}(q^2)] \right. \\ &\quad \left. + \frac{q^2}{2M_B} [h_{V_2}(q^2) - h_{V_3}(q^2)] \right\}. \end{aligned} \quad (28)$$

(c)  $B \rightarrow AV(^1P_1)$  transition

$H_i$  are obtained from expressions (28) by replacement of form factors  $h_i(q^2)$  by  $g_i(q^2)$ .

(d)  $B \rightarrow T(^3P_2)$  transition

$$H_\pm = \frac{\lambda^{1/2}}{2\sqrt{2}M_B M_T} \left[ (M_B + M_T) t_{A_1}(q^2) \pm \frac{\lambda^{1/2}}{M_B + M_T} t_V \right],$$

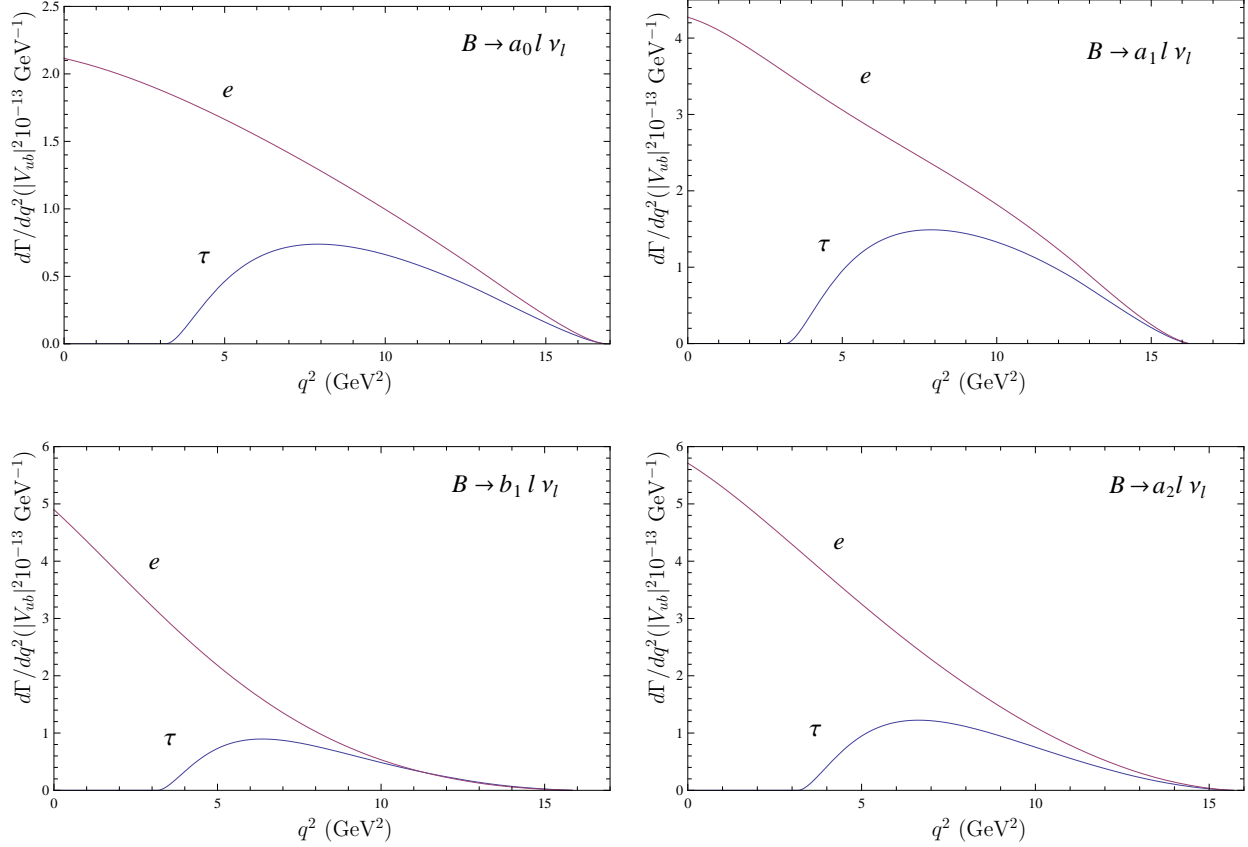


FIG. 5: Predictions for the differential decay rates (in  $|V_{ub}|^2 10^{-13} \text{ GeV}^{-1}$ ) of the  $B$  semileptonic decays to the  $P$ -wave light mesons.

$$\begin{aligned}
 H_0 &= \frac{\lambda^{1/2}}{2\sqrt{6}M_B M_T^2 \sqrt{q^2}} \left\{ (M_B + M_T)(M_B^2 - M_T^2 - q^2)t_{A_1}(q^2) + \frac{\lambda}{2M_B} [t_{A_2}(q^2) + t_{A_3}(q^2)] \right\}, \\
 H_t &= \sqrt{\frac{2}{3}} \frac{\lambda}{4M_B M_T^2 \sqrt{q^2}} \left\{ (M_B + M_T)t_{A_1}(q^2) + \frac{M_B^2 - M_T^2}{2M_B} [t_{A_2}(q^2) + t_{A_3}(q^2)] \right. \\
 &\quad \left. + \frac{q^2}{2M_B} [t_{A_2}(q^2) - t_{A_3}(q^2)] \right\}. \tag{29}
 \end{aligned}$$

Here the subscripts  $\pm, 0, t$  denote transverse, longitudinal and time helicity components, respectively.

Now we substitute the weak decay form factors calculated in the previous section in the above expressions for decay rates. The resulting differential distributions for the  $B$  decays to the  $P$ -wave light mesons are plotted in Fig. 5. The corresponding total decay rates are obtained by integrating the differential decay rates over  $q^2$ . For calculations we use the following value of the CKM matrix element  $|V_{ub}| = 0.0038 \pm 0.00044$  [1]. It is necessary to point out that the kinematical range accessible in these semileptonic decays is rather broad. Therefore the knowledge of the  $q^2$  dependence of the form factors is very important for reducing theoretical uncertainties of the decay rates. Our results for the semileptonic

TABLE IV: Predictions for the decay rates of the semileptonic  $B$  decays to the  $P$ -wave light mesons (in  $|V_{ub}|^2 \text{ps}^{-1}$ ).

Decay	$\Gamma(l = e, \mu)$	$\Gamma(l = \tau)$
$B \rightarrow a_0 l \nu$	3.18	1.00
$B \rightarrow a_1 l \nu$	5.90	1.95
$B \rightarrow b_1 l \nu$	4.04	0.91
$B \rightarrow a_2 l \nu$	5.77	1.27

TABLE V: Comparison of theoretical predictions for the branching ratios of the semileptonic  $B$  decays to the  $P$ -wave light mesons (in  $10^{-5}$ ). EFG: Ebert, Faustov, Galkin, this paper.

Decay	EFG	ISGW2 [18]	pQCD [19]	LCSR [20]	SR [21]
$\bar{B}^0 \rightarrow a_0^+ e \nu$	$7.0 \pm 2.8$	7.3	$32.5^{+23.6}_{-13.6}$	$18^{+9}_{-6}$	
$\bar{B}^0 \rightarrow a_0^+ \tau \nu$	$2.2 \pm 0.9$		$13.2^{+9.7}_{-5.7}$	$6.3^{+3.4}_{-2.5}$	
$\bar{B}^0 \rightarrow a_1^+ e \nu$	$13.0 \pm 5.2$	19.2	$29.6^{+17.4}_{-13.9}$	$30.2^{+10.3}_{-10.3}$	16
$\bar{B}^0 \rightarrow a_1^+ \tau \nu$	$4.3 \pm 1.7$		$13.4^{+7.8}_{-6.3}$		
$\bar{B}^0 \rightarrow b_1^+ e \nu$	$8.9 \pm 3.6$	24.1	$28.8^{+15.1}_{-12.2}$	$19.3^{+8.4}_{-6.8}$	
$\bar{B}^0 \rightarrow b_1^+ \tau \nu$	$2.0 \pm 0.8$		$12.6^{+6.6}_{-5.4}$		
$\bar{B}^0 \rightarrow a_2^+ e \nu$	$12.7 \pm 5.1$	1.1	$11.6^{+8.1}_{-5.7}$	16	
$\bar{B}^0 \rightarrow a_2^+ \tau \nu$	$2.8 \pm 1.1$		$4.1^{+2.9}_{-2.0}$	6	

$B$  decay rates to the  $P$ -wave light mesons are given in Table IV.<sup>2</sup> The errors of the decay rates presented in this table originate from the form factor uncertainties, discussed in the previous section, and are about 7%.

The predictions for the branching ratios of the semileptonic  $B$  decays to the  $P$ -wave light meson states<sup>3</sup> are compared with the previous calculations [18–21] in Table V. The authors of Refs. [18] use the constituent quark (ISGW2) model. Perturbative QCD (pQCD) approach is adopted in Ref. [19]. Calculations in Ref. [20] are based on the light-cone QCD sum rules (LCSR), while Ref. [21] employs the QCD sum rules. Our predictions for  $B \rightarrow a_{0,1}(b_1)l\nu$  decays are somewhat lower than the central values of pQCD and LCSR, but they are consistent within rather large errors of the considered approaches. The predicted central values of the branching ratio for the  $B \rightarrow a_2 l \nu$  decay are close in all calculations except the ISGW2 model, which predicts an order of magnitude lower value. Therefore we find that essentially different theoretical approaches give the values for the  $B \rightarrow a_J(b_1)l\nu$  decay branching ratios of order of  $10^{-4}$  which is the same as for the decays to the ground state  $\pi$  and  $\rho$  mesons. It is important to verify these predictions experimentally.

<sup>2</sup> We used the calculated value of the  $a_0$  mass from Table I.

<sup>3</sup> The presented errors of our calculations arise from the theoretical uncertainties in form factor calculations and experimental uncertainties which mainly originate from the rather poor knowledge of the CKM matrix element  $V_{ub}$ . The latter uncertainty is dominant.

## VI. NONLEPTONIC DECAYS

In the standard model nonleptonic  $B$  decays are described by the effective Hamiltonian, obtained by integrating out the heavy  $W$ -boson and top quark. For  $\Delta B = 1$  transitions ( $q = d, s$ ) [22]

$$H_{\text{eff}} = \frac{G_F}{\sqrt{2}} \left\{ V_{cb}V_{cq}^* [c_1(\mu)O_1^c + c_2(\mu)O_2^c] + V_{ub}V_{uq}^* [c_1(\mu)O_1^u + c_2(\mu)O_2^u] - V_{tb}V_{tq}^* \sum_{i=3}^{10} c_i(\mu)O_i(\mu) \right\}. \quad (30)$$

The Wilson coefficients  $c_i(\mu)$  are evaluated perturbatively at the  $W$  scale and then are evolved down to the renormalization scale  $\mu \approx m_b$  by the renormalization-group equations. The expressions  $O_i$  are local four-quark operators which are given by

$$\begin{aligned} O_1^{q'} &= (\bar{q}'b)_{V-A}(\bar{q}q')_{V-A}, \\ O_2^{q'} &= (\bar{q}'b_j)_{V-A}(\bar{q}_j q'_i)_{V-A}, \\ O_{3(5)} &= (\bar{q}b)_{V-A} \sum_{q'} (\bar{q}'q')_{V-A,(V+A)}, \\ O_{4(6)} &= (\bar{q}_i b_j)_{V-A} \sum_{q'} (\bar{q}'_j q'_i)_{V-A,(V+A)}, \\ O_{7(9)} &= \frac{3}{2}(\bar{q}b)_{V-A} \sum_{q'} e_{q'} (\bar{q}'q')_{V+A,(V-A)}, \\ O_{8(10)} &= \frac{3}{2}(\bar{q}_i b_j)_{V-A} \sum_{q'} e_{q'} (\bar{q}'_j q'_i)_{V+A,(V-A)}, \end{aligned} \quad (31)$$

where  $e_q$  denotes the quark electric charge and the following notations are used

$$(\bar{q}q')_{V\mp A} = \bar{q}\gamma_\mu(1 \mp \gamma_5)q'.$$

The nonleptonic two-body decay amplitude of a  $B$  meson into light mesons can be expressed through the matrix element of the effective weak Hamiltonian  $H_{\text{eff}}$ <sup>4</sup>

$$\begin{aligned} M(B \rightarrow M_1 M_2) = \langle M_1 M_2 | H_{\text{eff}} | B \rangle &= \frac{G_F}{\sqrt{2}} \left\{ V_{ub}V_{uq}^* [c_1 \langle M_1 M_2 | O_1^u | B \rangle + c_2 \langle M_1 M_2 | O_2^u | B \rangle] \right. \\ &\quad \left. - V_{tb}V_{tq}^* \sum_{i=3}^{10} c_i \langle M_1 M_2 | O_i(\mu) | B \rangle \right\}. \end{aligned} \quad (32)$$

The factorization approach, which is extensively used for the calculation of two-body nonleptonic decays assumes that the nonleptonic decay amplitude reduces to the product of a meson transition matrix element and a decay constant [24]. This assumption in general cannot be exact. However, it is expected that factorization can hold for energetic decays, where both final mesons are light and therefore possess large recoil momenta [25]. A justification of this assumption is usually based on the issue of color transparency [26]. In these decays the

<sup>4</sup> Since we make all further calculation adopting the naive factorization assumption we neglect contributions of charming penguins [23] which are absent in this approximation.

final hadrons, which have a large relative momentum, are produced in the form of almost point-like color-singlet objects that do not couple to soft gluons at leading order. Therefore they undergo only hard interactions with the  $B$  meson remnants before they hadronize. A more general treatment of factorization is given in Refs. [27] where it is shown that its naive form follows in the heavy quark limit at zeroth order in  $\alpha_s$  and  $\Lambda_{\text{QCD}}/m_B$ .

Then the decay amplitude can be approximated by the product of one-particle matrix elements, e.g., the tree part of the matrix element ( $q = d, s$ ) is given by

$$\begin{aligned} \langle M_1^0 M_2^- | c_1 O_1 + c_2 O_2 | B^- \rangle &\approx a_1 \langle M_1^0 | (\bar{u}b)_{V-A} | B^- \rangle \langle M_2^- | (\bar{q}u)_{V-A} | 0 \rangle \\ &+ a_2 \langle M_2^- | (\bar{q}b)_{V-A} | B^- \rangle \langle M_1^0 | (\bar{u}u)_{V-A} | 0 \rangle, \end{aligned} \quad (33)$$

in which the Wilson coefficients appear in the following linear combinations

$$\begin{aligned} a_i &= c_i + \frac{1}{N_c} c_{i+1} \quad (i = \text{odd}) \\ a_i &= c_i + \frac{1}{N_c} c_{i-1} \quad (i = \text{even}) \end{aligned} \quad (34)$$

and  $N_c$  is the number of colors. For calculations we use the values of the next-to-leading order Wilson coefficients obtained in Ref. [22] for  $\Lambda_{\overline{\text{MS}}}^{(5)} = 225$  MeV in the HV ('t Hooft-Veltman) scheme:  $c_1 = 1.105$ ,  $c_2 = -0.228$ ,  $c_3 = 0.013$ ,  $c_4 = -0.029$ ,  $c_5 = 0.009$ ,  $c_6 = -0.033$ ,  $c_7/\alpha = 0.005$ ,  $c_8/\alpha = 0.060$ ,  $c_9/\alpha = -1.283$ ,  $c_{10}/\alpha = 0.266$ , where  $\alpha$  is the fine structure constant.

The matrix elements of the weak current  $\langle M | (\bar{q}b)_{V-A} | B \rangle$  between  $B$  and light meson states are expressed through the decay form factors (see, e.g., (18)-(22)). The matrix element  $\langle M | (\bar{q}_1 q_2)_{V-A} | 0 \rangle$  between vacuum and a final pseudoscalar ( $P$ ), vector ( $V$ ), scalar ( $S$ ) and axial vector ( $AV$ ) meson is parametrized by the decay constants  $f_{P,V,S,AV}$

$$\begin{aligned} \langle P | \bar{q}_1 \gamma^\mu \gamma_5 q_2 | 0 \rangle &= i f_P p_P^\mu, \\ \langle V | \bar{q}_1 \gamma_\mu q_2 | 0 \rangle &= \epsilon_\mu M_V f_V, \\ \langle S | \bar{q}_1 \gamma^\mu q_2 | 0 \rangle &= f_S p_P^\mu, \\ \langle AV | \bar{q}_1 \gamma_\mu \gamma_5 q_2 | 0 \rangle &= \epsilon_\mu M_{AV} f_{AV}, \end{aligned} \quad (35)$$

while the corresponding matrix element for the tensor ( $T$ ) meson vanishes since

$$\langle T | \bar{q}_1 \gamma_\mu q_2 | 0 \rangle \propto \epsilon_{\mu\nu} p^\nu = 0, \quad (36)$$

due to the properties of the polarization tensor  $\epsilon_{\mu\nu}$ . The pseudoscalar  $f_P$  and vector  $f_V$  decay constants were calculated within our model in Ref. [28]. It was shown that the complete account of relativistic effects is necessary to get agreement with experiment for decay constants especially of light mesons. The scalar decay constant is proportional to the difference of the light quark masses and thus exactly vanishes for the neutral scalar mesons and also vanishes for the charged ones if isospin symmetry is assumed,  $f_{a_0^\pm} \approx f_{a_0^0} = f_{f_0} = 0$ . The axial vector  $b_1$  ( $^1P_1$ ) meson cannot be produced from the vacuum by the axial vector current due to the  $G$ -parity conservation and, therefore,  $f_{b_1} = 0$ . We use the following

values of the decay constants:  $f_\pi = 0.131$  GeV,  $f_\rho = 0.220$  GeV,  $f_K = 0.160$  GeV,  $f_{K^*} = 0.220$  GeV,  $f_\phi = 0.240$  GeV and  $f_{a_1} = f_{f_1} = 0.238$  GeV. The relevant CKM matrix elements [1] are  $|V_{ud}| = 0.975$ ,  $|V_{us}| = 0.225$ ,  $|V_{ub}| = |0.0019 - i0.0033| = 0.0038$ ,  $|V_{tb}| = 0.999$ ,  $|V_{td}| = |0.0080 - i0.0032| = 0.0086$ ,  $|V_{ts}| = 0.0403$ .

The matrix elements of the weak current between the  $B$  meson and the final light meson entering the factorized nonleptonic decay amplitude (33) are parametrized by the set of decay form factors. Using the form factors obtained in Sec. IV and our previous results for  $B$  decays to the ground-state  $\pi$  and  $\rho$  mesons [6], we get predictions for the branching ratios of the nonleptonic  $B$  decay to orbitally excited light mesons and display them in Tables VI-IX in comparison with other calculations [29–40]<sup>5</sup> and available experimental data [1–5]. We can roughly estimate the error of our calculations within adopted naive factorization approach to be about 40%. It originates both from theoretical uncertainties in the form factor and effective Wilson coefficient calculations and experimental uncertainties in the values of CKM matrix elements (which are dominant), decay constants and meson masses.

The difference between charge combinations of the same final mesons in Tables VI-IX is sometimes enormous. It originates mainly from the different set of diagrams for the nonleptonic decay process involving charged and neutral light mesons. For example, decays  $\bar{B}^0 \rightarrow a_{0,2}^+ K^-$  and  $B^- \rightarrow a_{0,2}^0 K^-$  are tree dominated, while decays  $\bar{B}^0 \rightarrow a_{0,2}^0 K^0$  and  $B^- \rightarrow a_{0,2}^- K^0$  are penguin dominated. In the case of the decays involving the axial vector  $a_1$  meson the situation is more complicated since its decay constant is not equal to zero and thus additional diagrams, where  $a_1$  is produced by the weak current from the vacuum, contribute to the nonleptonic decay amplitudes. It is also necessary to take into account additional factors arising from the composition of neutral light unflavored mesons [e.g.,  $a_i^0 = 1/\sqrt{2}(d\bar{d} - u\bar{u})$ ,  $i = 0, 1, 2$ ].

In Table VI we present predictions for the branching ratios of the two-body nonleptonic  $B$  decays involving the  $P$ -wave light scalar  $q\bar{q}$  meson  $a_0$ . We compare our results with predictions of LCSR [29], QCD factorization with the form factors evaluated in the light-front quark model [30], naive factorization with form factors obtained using QCD sum rules [31], and pQCD [32] approach. We see that LCSR [29] and pQCD [32] give the branching fractions which are almost an order of magnitude larger than our predictions. This is the consequence of significantly larger values of the form factors  $f_+^{Ba_0}(0) = 0.46$  in LCSR [29] and  $f_+^{Ba_0}(0) = 0.86$  in pQCD [32] approaches compared to our result  $f_+^{Ba_0}(0) = 0.27$ . On the other hand, our predictions are consistent with the ones of [30] and [31] which both use  $f_+^{Ba_0}(0) = 0.26$ . In Ref. [30] it was argued that the two-body nonleptonic  $B$  decay rates involving light scalars are significantly different in two- and four-quark pictures of these mesons. Therefore experimental measurement of these nonleptonic decay rates can discriminate between different models for form factors and help to clarify the nature of light scalars. At present only experimental upper limits [2] are available for two  $\bar{B}^0$  decay modes to the scalar  $a_0(1450)$  and charged pion or kaon, but unfortunately they involve the unmeasured branching ratio  $\mathcal{B}(a_0(1450) \rightarrow \eta\pi)$ .

In Tables VII and VIII we compare theoretical predictions for the two-body nonleptonic  $B$  decays involving the axial vector  $a_1$  and  $b_1$  light mesons with available experimental data. Naive factorization hypothesis and decay form factors calculated within the ISGW2 model are used in Ref. [33]. In Ref. [34] these decays are investigated in the framework of QCD factorization with the light cone distribution amplitudes evaluated using QCD sum rules.

---

<sup>5</sup> Only central values are given for all theoretical predictions which have rather large error bars.

TABLE VI: The branching ratios of the two-body nonleptonic  $B$  decays involving the scalar  $1^3P_0$  light mesons (in  $10^{-6}$  ).

Decay	EFG	[29]	[30]	[31]	[32]	Exp. [1, 2]
$\bar{B}^0 \rightarrow a_0^+ \pi^-$	3.6	20	3.1	8		$< 2.3/\mathcal{B}(a_0 \rightarrow \eta\pi)$
$\bar{B}^0 \rightarrow a_0^0 \pi^0$	0.03		0.7			
$B^- \rightarrow a_0^0 \pi^-$	2.0		2.5	4		
$B^- \rightarrow a_0^- \pi^0$	0.07		1.1	0.01		
$\bar{B}^0 \rightarrow a_0^+ K^-$	0.29		0.3	1		$< 3.1/\mathcal{B}(a_0 \rightarrow \eta\pi)$
$\bar{B}^0 \rightarrow a_0^0 K^0$	0.02		0.1			
$B^- \rightarrow a_0^- K^0$	0.04		0.1			
$B^- \rightarrow a_0^0 K^-$	0.15		0.2	0.5		
$\bar{B}^0 \rightarrow a_0^+ \rho^-$	10.3	38	13.3			
$\bar{B}^0 \rightarrow a_0^0 \rho^0$	0.05		3.2			
$B^- \rightarrow a_0^0 \rho^-$	5.5		25.4			
$B^- \rightarrow a_0^- \rho^0$	0.10		4.5			
$\bar{B}^0 \rightarrow a_0^+ K^{*-}$	2.0		5.3		28	
$\bar{B}^0 \rightarrow a_0^0 K^{*0}$	0.35		2.7		14	
$B^- \rightarrow a_0^0 K^{*-}$	1.1		2.6		7.0	
$B^- \rightarrow a_0^- K^{*0}$	0.8		7.8		30	
$\bar{B}^0 \rightarrow a_0^+ a_1^-$	11.4					
$\bar{B}^0 \rightarrow a_0^0 a_1^0$	0.05					
$B^- \rightarrow a_0^- a_1^0$	0.11					
$B^- \rightarrow a_0^0 a_1^-$	6.1					

The authors of Ref. [35] employ naive factorization and additional input of a limited number of experimental data <sup>6</sup>, while pQCD and soft collinear effective theory (SCET), with form factors being fitted parameters, are applied in Ref. [36]. The two-body nonleptonic  $B$  decays involving axial vector light mesons are the best studied experimentally among the decays to excited light mesons. Values or upper limits are available for almost a half of the decays given in Tables VII, VIII. Notwithstanding rather large experimental error bars the existing data can already discriminate between various theoretical approaches. As it is seen from these tables our results and predictions of Refs. [34], [35], [36] (pQCD and SCET) are consistent with each other (taking into account rather large error bars) for the most decay branching ratios and agree with the available experimental data. While the results of Ref. [33] are in most cases significantly different and seem to be ruled out by experiment.

In Table IX our predictions for the branching ratios of the two-body nonleptonic  $B$  decays involving tensor  $a_2$  and  $f_2$  light mesons are confronted with other theoretical predictions and experimental data. References [37] and [38] employ generalized factorization complemented by form factors calculated in the nonrelativistic ISGW model and covariant light-front approach, respectively. The authors of Ref. [39] apply the QCD factorization, while naive

<sup>6</sup> Two possible values of the  $K_1(1270)$  and  $K_1(1400)$  mixing angle are considered in Ref. [35]. In Tables VII and VIII we present results only for its preferred value  $58^\circ$ .



TABLE VII: The branching ratios of the two-body nonleptonic  $B$  decays involving the axial vector  $1^3P_1$  light mesons (in  $10^{-6}$ ).

Decay	EFG	[33]	[34]	[35]	pQCD [36]	[36]	Exp. [1, 3]
$\bar{B}^0 \rightarrow a_1^+ \pi^-$	15.7	74.3	9.1	11.8	12.7	10.7	$13.0 \pm 4.3$
$\bar{B}^0 \rightarrow a_1^- \pi^+$	21.1	36.7	23.4	12.3	15.7	17.0	$24.2 \pm 5.8$
$\bar{B}^0 \rightarrow a_1^\pm \pi^\pm$	36.8	111.0	32.5	24.1	28.3	27.7	$33 \pm 5$
$\bar{B}^0 \rightarrow a_1^0 \pi^0$	0.34	0.27	0.9	1.7	0.12	5.5	$< 1100$
$B^- \rightarrow a_1^0 \pi^-$	11.3	43.2	7.6	8.8	6.7	17.2	$20.4 \pm 4.7 \pm 3.4$
$B^- \rightarrow a_1^- \pi^0$	13.7	13.6	14.4	10.6	8.1	19.0	$13.2 \pm 2.7 \pm 2.1$
$\bar{B}^0 \rightarrow a_1^+ K^-$	13.2	72.2	18.3	41	20.6	15.8	$16.3 \pm 2.9 \pm 2.3$
$\bar{B}^0 \rightarrow a_1^0 K^0$	6.0	42.3	6.9	25	8.0	6.3	
$B^- \rightarrow a_1^- K^0$	19.8	84.1	21.6	52	25.5	15.5	$33.2 \pm 5.0 \pm 4.4$
$B^- \rightarrow a_1^0 K^-$	14.3	43.4	13.9	28	15.4	10.5	
$\bar{B}^0 \rightarrow a_1^+ \rho^-$	20.7	4.3	23.9				$< 61$
$\bar{B}^0 \rightarrow a_1^+ K^{*-}$	3.9	0.92	10.6				
$B^- \rightarrow a_1^- K^{*0}$	0.66	0.51	11.2				$1.3^{+1.1+1.1}_{-1.0-2.6}$
$\bar{B}^0 \rightarrow a_1^0 \phi$	0.001	0.0005	0.01				
$\bar{B}^0 \rightarrow a_1^+ a_1^-$	46.1	6.4	37.4				$47.3 \pm 10.5 \pm 6.3$
$\bar{B}^0 \rightarrow a_1^0 a_1^0$	0.81	0.1	0.5				
$B^- \rightarrow a_1^- a_1^0$	31.5	3.6	22.4				$< 13000$
$\bar{B}^0 \rightarrow a_1^0 f_1$	0.85	0.02	0.1				
$B^- \rightarrow a_1^- f_1$	17.9	3.7	12.4				
$\bar{B}^0 \rightarrow f_1 \pi^0$	0.56	0.47	0.26				
$B^- \rightarrow f_1 \pi^-$	11.6	34.1	5.2				
$\bar{B}^0 \rightarrow f_1 K^0$	2.9	34.7	14.6				
$B^- \rightarrow f_1 K^-$	4.9	31.1	14.8				$< 2.0$

factorization and the improved ISGW2 model are used in Ref. [40]. From this table we see that theoretical predictions strongly depend on the adopted approach and the model for form factors. Experimental data are available only for a few considered decay modes and represent mostly upper limits. The measurements [5] were recently carried out for two charged  $B$  decays involving the tensor  $f_2$  meson and the charged pion and kaon as well as for one neutral  $B$  decay to  $f_2$  and  $K^0$ . Our model prediction for  $B^- \rightarrow f_2 K^-$  is in agreement with experiment, while the ones for  $\bar{B}^0 \rightarrow f_2 K^0$  and for  $B^- \rightarrow f_2 \pi^-$  are lower and larger than experimental values, respectively. However experimental errors are still large in order to make definite conclusions.

## VII. CONCLUSIONS

Weak form factors of the  $B$  mesons decays to the first orbital excitations of light mesons were calculated in the framework of the QCD-motivated relativistic quark model. The form factor dependence on the momentum transfer was selfconsistently determined in the whole

TABLE VIII: The branching ratios of the two-body nonleptonic  $B$  decays involving the axial vector  $1^1P_1$  light mesons (in  $10^{-6}$ ). All experimental values include the unmeasured branching ratios  $\mathcal{B}(b_1 \rightarrow \omega\pi)$ .

Decay	EFG	[33]	[34]	[35]	pQCD [36]	[36]	Exp. [1, 4]
$\bar{B}^0 \rightarrow b_1^+ \pi^-$	17.7	36.2	11.2	0.7	18.7	7.7	
$\bar{B}^0 \rightarrow b_1^- \pi^+$	0	0	0.3	$\approx 0$	1.4	0.6	
$\bar{B}^0 \rightarrow b_1^\pm \pi^\pm$	17.7	36.2	11.5	0.7	20.2	8.3	$10.9 \pm 1.2 \pm 0.9$
$\bar{B}^0 \rightarrow b_1^0 \pi^0$	0.18	0.15	1.1	0.01	1.5	1.8	$0.4 \pm 0.8 \pm 0.2$
$B^- \rightarrow b_1^0 \pi^-$	9.5	18.6	9.6	0.7	5.1	5.0	$6.7 \pm 1.7 \pm 1.0$
$B^- \rightarrow b_1^- \pi^0$	0.62	0.29	0.4	0.5	1.0	2.0	$1.8 \pm 0.9 \pm 0.2$
$\bar{B}^0 \rightarrow b_1^+ K^-$	11.6	35.7	12.1	2.0	42.9	8.5	$7.4 \pm 1.0 \pm 1.0$
$\bar{B}^0 \rightarrow b_1^0 K^0$	4.4	19.3	7.3	4.0	23.3	4.0	$5.1 \pm 1.8 \pm 0.5$
$B^- \rightarrow b_1^- K^0$	8.3	41.5	14.0	3.0	55.0	8.6	$9.6 \pm 1.7 \pm 0.9$
$B^- \rightarrow b_1^0 K^-$	8.2	18.1	6.2	0.7	24.9	4.6	$9.1 \pm 1.7 \pm 1.0$
$\bar{B}^0 \rightarrow b_1^+ \rho^-$	22.7	1.6	32.1				
$\bar{B}^0 \rightarrow b_1^0 \rho^0$	0.20	0.002	3.2				$< 3.4$
$B^- \rightarrow b_1^- \rho^0$	0.43	0.0005	0.9				$< 5.2$
$B^- \rightarrow b_1^0 \rho^-$	11.2	0.86	29.1				$< 3.3$
$\bar{B}^0 \rightarrow b_1^+ K^{*-}$	4.1	0.32	12.5				
$\bar{B}^0 \rightarrow b_1^0 K^{*0}$	0.36	0.15	6.4				$< 8.0$
$B^- \rightarrow b_1^0 K^{*-}$	2.2	0.12	12.8				$< 6.7$
$B^- \rightarrow b_1^- K^{*0}$	0.7	0.18	7.0				$< 5.9$
$\bar{B}^0 \rightarrow b_1^0 \phi$	0.001	0.0002	0.01				
$\bar{B}^0 \rightarrow b_1^+ b_1^-$	0	0	1.0				
$\bar{B}^0 \rightarrow b_1^0 b_1^0$	0	0	3.2				
$B^- \rightarrow b_1^- b_1^0$	0	0	1.4				
$\bar{B}^0 \rightarrow h_1 \pi^0$	0.22	0.16	0.16				
$B^- \rightarrow h_1 \pi^-$	9.6	18.6	1.8				
$\bar{B}^0 \rightarrow h_1 K^0$	4.3	19.0	10.9				
$B^- \rightarrow h_1 K^-$	11.1	19.0	11.3				

accessible kinematical range without applying any additional parameterizations and extrapolations. All relativistic contributions, including contributions of the intermediate negative-energy states and transformations of the wave functions to the moving reference frame were consistently taken into account. This significantly reduces theoretical uncertainties of the obtained form factors.

On this basis the branching ratios of the  $B$  semileptonic decays to orbitally excited light mesons were calculated. Our predictions were compared with other theoretical calculations based on the ISGW2 quark model [18], perturbative QCD [19], light cone sum rules [20] and QCD sum rules [21]. It is important to point out that in most of the previous approaches the weak form factors were calculated in some particular kinematical point or limited kinematical range and then were extrapolated to the whole accessible kinematical range, which is rather broad for such decays. Thus the ISGW2 quark model allows the calculation of

TABLE IX: The branching ratios of the two-body nonleptonic  $B$  decays involving the tensor  $1^3P_2$  light mesons (in  $10^{-6}$ ).

Decay	EFG	[37]	[38]	[39]	[40]	Exp. [1, 5]
$\bar{B}^0 \rightarrow a_2^+ \pi^-$	9.8	4.9	8.19	5.2	13.0	< 300
$\bar{B}^0 \rightarrow a_2^0 \pi^0$	0.009	0.0003	0.007	0.24	0.18	
$B^- \rightarrow a_2^0 \pi^-$	5.2	2.6	4.38	3.0	6.7	
$B^- \rightarrow a_2^- \pi^0$	0.19	0.001	0.015	0.24	0.38	
$\bar{B}^0 \rightarrow a_2^+ K^-$	1.6	0.58	0.73	9.7	0.95	
$\bar{B}^0 \rightarrow a_2^0 K^0$	0.02	0.005	0.014	4.2		
$B^- \rightarrow a_2^- K^0$	0.05	0.011	0.015	8.4		
$B^- \rightarrow a_2^0 K^-$	1.0	0.31	0.39	4.9	0.51	< 45
$\bar{B}^0 \rightarrow a_2^+ \rho^-$	27.1	14.7	36.2	11.3	36.2	
$\bar{B}^0 \rightarrow a_2^0 \rho^0$	0.23	0.003	0.03	0.39	0.5	
$B^- \rightarrow a_2^0 \rho^-$	14.6	7.3	19.3	8.4	19.4	
$B^- \rightarrow a_2^- \rho^0$	0.51	0.007	0.071	0.82	1.1	< 720
$\bar{B}^0 \rightarrow a_2^+ K^{*-}$	5.0	3.5	7.25	6.1	1.9	
$\bar{B}^0 \rightarrow a_2^0 K^{*0}$	0.9	2.1	4.0	3.4		
$B^- \rightarrow a_2^- K^{*0}$	1.8	4.5	8.6	6.1		
$B^- \rightarrow a_2^0 K^{*-}$	2.7	1.9	2.8	2.9	1.0	
$\bar{B}^0 \rightarrow a_2^+ a_1^-$	59.0		42.5			
$\bar{B}^0 \rightarrow a_2^0 a_1^0$	0.32		0.04			
$B^- \rightarrow a_2^- a_1^0$	0.69		0.085			
$B^- \rightarrow a_2^0 a_1^-$	31.6		22.7			
$\bar{B}^0 \rightarrow f_2 \pi^0$	0.09	0.0003		0.15	0.19	
$B^- \rightarrow f_2 \pi^-$	5.1	2.8		2.7	7.1	$1.57 \pm 0.42 \pm 0.16_{-0.19}^{+0.53}$
$\bar{B}^0 \rightarrow f_2 K^0$	0.11	0.005		3.4		$2.7_{-0.8}^{+1.9} \pm 0.9$
$B^- \rightarrow f_2 K^-$	1.0	0.34		3.8	0.54	$1.33 \pm 0.30 \pm 0.11_{-0.32}^{+0.20}$

the form factors at  $q^2 = q_{\text{max}}^2$  and then applies the Gaussian parameterization for them, while light cone sum rules determine form factors in the range near  $q^2 = 0$  and, therefore, require extrapolation. It was found that all these essentially different approaches predict that semileptonic decays to orbitally excited light mesons have branching ratios of order  $10^{-4}$  which is the same as for the decays to the ground state  $\pi$  and  $\rho$  mesons.

The obtained form factors were used for the evaluation of the branching ratios of the two-body nonleptonic decays of  $B$  mesons involving orbitally excited light mesons. The factorization approach was employed to express the decay matrix elements through the products of the weak form factors and decay constants. Decays involving scalar  $a_0(1450)$ ,<sup>7</sup> axial vector  $a_1(1260)$ ,  $f_1(1285)$ ,  $b_1(1235)$ ,  $h_1(1170)$  or tensor  $a_2(1320)$ ,  $f_2(1270)$  and light  $\pi$ ,  $\rho$ ,  $K$  and  $K^*$  mesons were considered. Obtained predictions were compared with previous calculations based on naive and generalized factorization with form factors obtained in dif-

<sup>7</sup> Under the assumption that it is the  $1^3P_0$   $q\bar{q}$  state.

ferent models, QCD factorization, light cone sum rules and perturbative QCD. It was found that the results significantly depend on the adopted approach for the calculation of the decay matrix elements and form factors. Our predictions agree well with the experimental data, which are mostly available for the decays involving axial vector light mesons, while some of the previous calculations significantly deviate from experimental values. Future more precise and comprehensive data, especially on the semileptonic decays, can help to discriminate between various theoretical approaches and form factor models.

### Acknowledgments

The authors are grateful to M. Müller-Preussker for support and to V. Matveev, V. Savrin and M. Wagner for discussions. Two of us (R.N.F. and V.O.G.) acknowledge the support by the *Deutsche Forschungsgemeinschaft* under contract Eb 139/6-1.

- 
- [1] K. Nakamura [Particle Data Group], *J. Phys. G* **37**, 075021 (2010).
  - [2] B. Aubert *et al.* [BABAR Collaboration], *Phys. Rev. D* **75**, 111102 (2007).
  - [3] B. Aubert *et al.* [BABAR Collaboration], *Phys. Rev. Lett.* **98**, 181803 (2007); *Phys. Rev. Lett.* **99**, 261801 (2007); *Phys. Rev. Lett.* **100**, 051803 (2008); *Phys. Rev. D* **80**, 092007 (2009); P. del Amo Sanchez *et al.* [The BABAR Collaboration], *Phys. Rev. D* **82**, 091101 (2010).
  - [4] B. Aubert *et al.* [The BABAR Collaboration], *Phys. Rev. Lett.* **99**, 241803 (2007); *Phys. Rev. D* **78**, 011104 (2008); *Phys. Rev. D* **80**, 051101 (2009).
  - [5] A. Garmash *et al.* [Belle Collaboration], *Phys. Rev. Lett.* **96**, 251803 (2006); B. Aubert *et al.* [BABAR Collaboration], *Phys. Rev. D* **78**, 012004 (2008); *Phys. Rev. D* **79**, 072006 (2009); *Phys. Rev. D* **80**, 112001 (2009).
  - [6] D. Ebert, R. N. Faustov and V. O. Galkin, *Phys. Rev. D* **75**, 074008 (2007).
  - [7] D. Ebert, R. N. Faustov and V. O. Galkin, *Phys. Rev. D* **79**, 114029 (2009).
  - [8] D. Ebert, R. N. Faustov and V. O. Galkin, *Eur. Phys. J. C* **60**, 273 (2009).
  - [9] D. Ebert, R. N. Faustov and V. O. Galkin, *Phys. Rev. D* **67**, 014027 (2003).
  - [10] D. Ebert, V. O. Galkin and R. N. Faustov, *Phys. Rev. D* **57**, 5663 (1998) [Erratum-*ibid.* *D* **59**, 019902 (1999)]; D. Ebert, R. N. Faustov and V. O. Galkin, *Eur. Phys. J. C* **66**, 197 (2010).
  - [11] R. N. Faustov and V. O. Galkin, *Z. Phys. C* **66**, 119 (1995).
  - [12] D. Ebert, R. N. Faustov and V. O. Galkin, *Phys. Rev. D* **73**, 094002 (2006).
  - [13] R. N. Faustov, *Ann. Phys.* **78**, 176 (1973); *Nuovo Cimento A* **69**, 37 (1970).
  - [14] D. Ebert, R. N. Faustov and V. O. Galkin, *Phys. Rev. D* **82**, 034019 (2010).
  - [15] J. Charles, A. Le Yaouanc, L. Oliver, O. Pene and J. C. Raynal, *Phys. Rev. D* **60**, 014001 (1999).
  - [16] D. Ebert, R. N. Faustov and V. O. Galkin, *Phys. Rev. D* **64**, 094022 (2001).
  - [17] M. A. Ivanov, J. G. Körner and P. Santorelli, *Phys. Rev. D* **71**, 094006 (2005) [Erratum-*ibid.* *D* **75**, 019901 (2007)].
  - [18] D. Scora and N. Isgur, *Phys. Rev. D* **52**, 2783 (1995).
  - [19] R. H. Li, C. D. Lu, W. Wang and X. X. Wang, *Phys. Rev. D* **79**, 014013 (2009); R. H. Li, C. D. Lu and W. Wang, *Phys. Rev. D* **79**, 034014 (2009); W. Wang, *Phys. Rev. D* **83**, 014008 (2011).

- [20] Y. M. Wang, M. J. Aslam and C. D. Lu, Phys. Rev. D **78**, 014006 (2008); K. C. Yang, Phys. Rev. D **78**, 034018 (2008); Z. G. Wang, arXiv:1011.3200 [hep-ph].
- [21] T. M. Aliev and M. Savci, Phys. Lett. B **456**, 256 (1999).
- [22] G. Buchalla, A. J. Buras and M. E. Lautenbacher, Rev. Mod. Phys. **68**, 1125 (1996).
- [23] M. Ciuchini, E. Franco, G. Martinelli and L. Silvestrini, Nucl. Phys. B **501**, 271 (1997).
- [24] M. Bauer, B. Stech, and M. Wirbel, Z. Phys. C **34**, 103 (1987).
- [25] M. J. Dugan and B. Grinstein, Phys. Lett. B **255**, 583 (1991).
- [26] J. D. Bjorken, Nucl. Phys. B (Proc. Suppl.) **11**, 325 (1989).
- [27] M. Beneke, G. Buchalla, M. Neubert and C. T. Sachrajda, Phys. Rev. Lett. **83**, 1914 (1999); Nucl. Phys. B **591**, 313 (2000).
- [28] D. Ebert, R. N. Faustov and V. O. Galkin, Phys. Lett. B **635**, 93 (2006).
- [29] V. Chernyak, Phys. Lett. B **509**, 273 (2001).
- [30] H. Y. Cheng, C. K. Chua and K. C. Yang, Phys. Rev. D **73**, 014017 (2006); Phys. Rev. D **77**, 014034 (2008).
- [31] D. Delepine, J. L. Lucio M., J. A. Mendoza S. and C. A. Ramirez, Phys. Rev. D **78**, 114016 (2008).
- [32] Z. Q. Zhang, Phys. Rev. D **83**, 054001 (2011).
- [33] G. Calderon, J. H. Munoz and C. E. Vera, Phys. Rev. D **76**, 094019 (2007).
- [34] H. Y. Cheng and K. C. Yang, Phys. Rev. D **76**, 114020 (2007); H. Y. Cheng and K. C. Yang, Phys. Rev. D **78**, 094001 (2008) [Erratum-ibid. D **79**, 039903 (2009)].
- [35] V. Laporta, G. Nardulli and T. N. Pham, Phys. Rev. D **74**, 054035 (2006) [Erratum-ibid. D **76**, 079903 (2007)].
- [36] W. Wang, R. H. Li and C. D. Lu, Phys. Rev. D **78**, 074009 (2008).
- [37] C. S. Kim, J. P. Lee and S. Oh, Eur. Phys. J. C **22**, 683 (2002); Eur. Phys. J. C **22**, 695 (2002); Phys. Rev. D **67**, 014002 (2003).
- [38] J. H. Munoz and N. Quintero, J. Phys. G **36**, 095004 (2009); J. Phys. G **36**, 125002 (2009).
- [39] H. Y. Cheng and K. C. Yang, Phys. Rev. D **83**, 034001 (2011).
- [40] N. Sharma, R. Dhir and R. C. Verma, Phys. Rev. D **83**, 014007 (2011).